Full paper/Mémoire

Rapid transfer of methyl red using calix[6]arene as a carrier in a bulk liquid membrane

Fakhar N. Memon, Shahabuddin Memon *, Fozia T. Minhas

National Centre of Excellence in Analytical Chemistry, University of Sindh, Jamshoro 76080, Pakistan

A B S T R A C T

In the present investigation, a calix[6]arene-based derivative (**1**) is employed as a selective carrier for the efficient transport of methyl red (MR) through bulk liquid membrane (BLM). Initially, the selectivity of **1** towards MR was confirmed among different dyes, such as methyl green (MG), methyl violate (MV), methylene blue (MB), methyl orange (MO), and eosin gelblich (EG) by liquid–liquid extraction experiments. Furthermore, the effect of the initial MR concentration of salts (NaCl, Na_2SO_4, and Na_2CO_3) and of the pH of the acceptor phase were also optimized using liquid–liquid extraction. Afterwards, the influence of basic parameters, such as carrier concentration in membrane phase, type of solvent, and stirring rate on MR transport was determined through BLM. Mass transfer of MR through BLM was analyzed by following the kinetic laws of two consecutive irreversible first-order reactions, and the kinetic parameters (k_1, k_2, R_m^{max}, t_{max}, J_d^{max}, J_a^{max}) were also calculated. Apparently, increase in membrane entrance (k_1) and exit rate (k_2) constants was accompanied by a rise in carrier concentration under a high stirring rate. In addition, CH_2Cl_2 proved to be a better solvent than $CHCl_3$ and CCl_4. The % transport of MR was 99% across the liquid membrane under optimized conditions. Real textile industrial wastewater samples gave also appreciable results in BLM under optimized conditions.

© 2013 Académie des sciences. Published by Elsevier Masson SAS. All rights reserved.

1. Introduction

Dyes are one of the major groups of chemicals that are responsible for the contamination of aquatic ecosystems. They are frequently used in a number of industries, such as leather, plastic, paper, rubber, textile and food coloring. From these industries, about 10,000 dyes, representing an annual production of 7×10^5 tons are commercially available, and up to 10% of them, used industrially, are lost as effluents. Even though, before discharging into wastewater, the industrial effluents are quite diluted, their intense color is the first sign of their presence as contaminants and small quantities are quite hazardous, not only for human beings, but also dangerous for aquatic

life. For example, some of the dyes are carcinogenic and may cause allergic dermatitis, skin irritation as well as mutation in man, and retard the proper transmission of sunlight to aquatic life [1]. A methyl red with molecular formula, $C_{15}H_{15}N_3O_2$, bearing an azo group is considered as carcinogenic. Student safety sheets for dyes and indicators classify methyl red as a harmful and irritating dye [2]. Since these dyes are stable to sunlight, wastewaters once contaminated with them are thus very difficult to treat with the traditional methods.

Consequently, numerous and versatile techniques have been developed and adopted successfully for dye-contaminated wastewater treatment, ranging from physicochemical to biological treatments [3], including nanofiltration [4], ionic liquid-based dispersive liquid–liquid extraction [5], adsorption [6], ionic liquid grafted magnetic nanoparticles [7] and oxidation–ozonation [8], etc. Some of these techniques may give good results; however, others do not

---

* Corresponding author.
   E-mail address: shahabuddinmemon@yahoo.com (S. Memon).
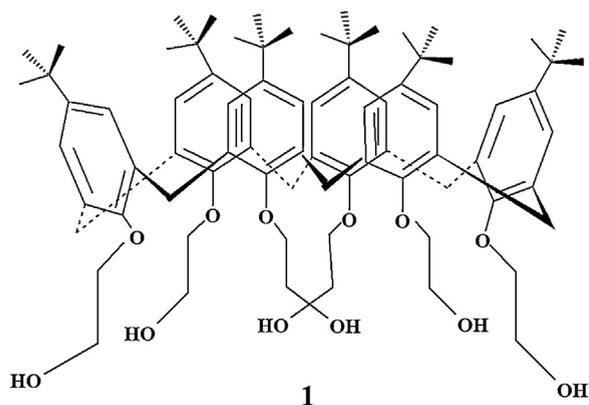
Fig. 1. Chemical structure of 5,11,17,23,29,35-hexa-*tert*-butyl-37,38,39,40,41,42-hexakis(2-hydroxyethoxy)calix[6]arene derivative (carrier **1**).

work at lower concentrations or often lead to treatment difficulties [9]. In this scenario, the existing literature on the use of bulk liquid membranes (BLM) for the transport of metal ions [10], phenols [11], drugs [12], and for the treatment of wastewater [13] is the clear justification of its efficiency, simplicity as well as sophistication. However, for dye removal, a little number of carriers has been utilized, such as mixture of D_2EHPA/M_2EHPA and sesame oil [14], TBAB [15], Cyanex 301 [16], cationic carrier [17], D_2EHPA [18], vegetable oil [19], Span 80 [20], and tri⁻dodecyl amine [21].

In this context, calixarenes are well-known macrocyclic receptors that have been widely utilized as efficient carriers for the transfer of metal ions [10,22,23]. Due to their unique cavity sizes, they are able to recognize the size of the guest molecules, and, consequently, to act as selective molecular recognizing agents in supramolecular systems. Therefore, by keeping in view the cavity size

concept of calixarene for molecular recognition, the present study is devoted to develop 5,11,17,23,29,35-hexa-*tert*-butyl-37,38,39,40,41,42-hexakis(2-hydroxyethoxy)-calix[6]arene (Fig. 1) as a highly efficient and rapid carrier to transport methyl red through a bulk liquid membrane. Consequently, the study explores the effect of solvent, stirring rate, and carrier concentration on the transport efficacy.

2. Experimental

2.1. Materials and methods

Analytical grade solvents were utilized to prepare the bulk liquid membrane. Deionized water passed through a Millipore Milli-Q Plus water purification system (Elga model classic UVF, UK) was used for the preparation of aqueous solutions. Salts (NaCl, Na_2CO_3 and Na_2SO_4) and dyes as shown in Fig. 2, including methyl green (MG), methyl red (MR), methyl violate (MV), methylene blue (MB), methyl orange (MO), and eosin gelblich (EG), were purchased from Merck. Compound (**1**) was synthesized according to a previously reported method [24] and 0.1 M NaOH/HCl solutions were used for pH adjustment.

2.2. Apparatus

A PerkinElmer (Shelton, CT 06484, USA) Lambda 35 UV–vis spectrophotometer was used to record UV–vis spectra. A pH meter (781-pH/Ion meter, Metrohm, Herisau, Switzerland) with a glass electrode and an internal reference electrode was used for pH adjustment. To set equal rotation rates of Teflon-coated magnetic bars, a Gallenkamp magnetic stirrer model APP SS610/5, UK was used. A Gallenkamp thermostat automatic mechanical shaker model BKS 305–101, UK was used for shaking. A U-type cell was used to perform transport experiments.
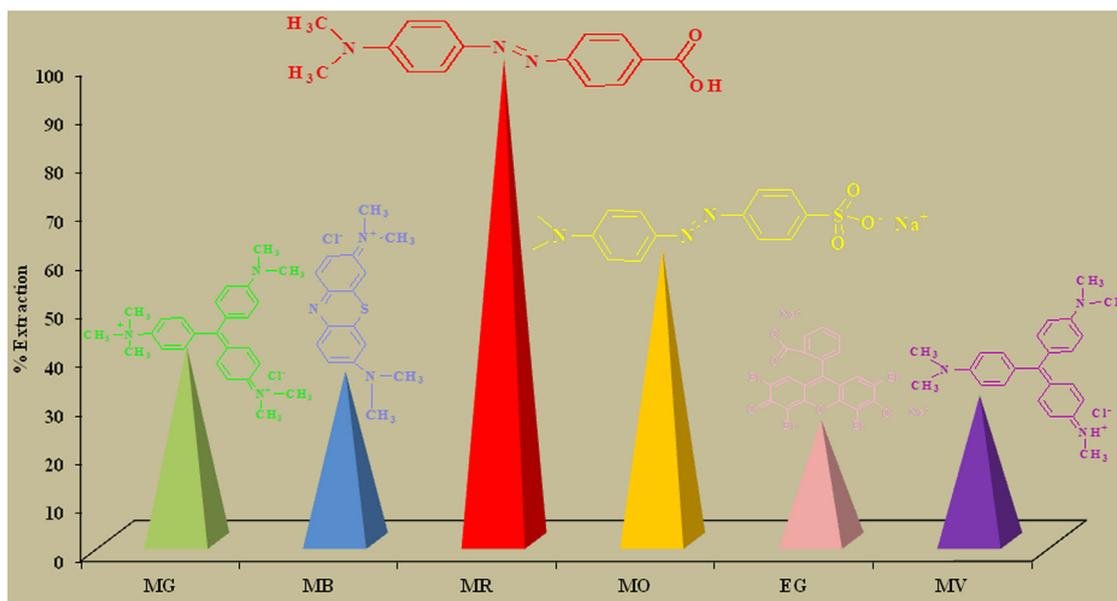
Fig. 2. (Color online.) Percentage extraction efficiency of carrier **1** for various dyes. Insets are the structures of different dyes.

2.3. Liquid–liquid extraction

According to Pederson's procedure [25], 10 mL of a 2.5×10^{-5} M dye solution was agitated with 10 mL of 1×10^{-3} M carrier **1** solution in chloroform at room temperature. The dye concentration was determined using the UV–visible spectrophotometer, whereas the extraction percent was calculated using the following equation:

$$E\% = \left[\frac{(C_0 - C)}{C_0}\right] \times 100 \tag{1}$$

where C_0 and C are the initial and final concentrations of dye in aqueous solution before and after extraction, respectively.

2.4. Liquid–liquid decomplexation

For the decomplexation of carrier **1** from the dye, the organic layer containing carrier (**1**) and the dye was taken and agitated with water at a pH varying from 2 to 12 at room temperature. The upper aqueous layer was taken and examined spectrophotometrically. The % of decomplexation was calculated using equation (2):

$$\%D = \frac{C_3}{C_1} \times 100 \tag{2}$$

where C_3 is the concentration of dye before extraction and C_1 is the concentration of dye released from the organic phase.

2.5. Bulk liquid membrane experiment

For BLM experiments, the organic phase containing carrier **1** (15 mL) was added at the bottom of a U-type cell, followed by careful addition of two portions of aqueous phases (10 mL). The surface area of the cell at the region of aqueous phases was 2.5 cm^2. The system was stirred at 800 rpm. The initial composition of the components of the cell was:

- organic phase = carrier **1** in chloroform (1×10^{-3} M);
- donor phase = dye solution (2.5×10^{-5} M);
- receiving phase = water at pH 12.

Equal portions of the samples from donor and receiving phases were taken simultaneously at regular time intervals, and dye concentration was examined spectrophotometrically.

3. Results and discussion

3.1. Liquid–liquid extraction

Primarily, the extraction efficiency/selectivity of the carrier **1** for the six different dyes (MG, MR, MV, MB, MO and EG) was evaluated by simple liquid–liquid extraction experiments. It is clear from Fig. 2 that carrier (**1**) shows excellent extraction efficiency for methyl red dye among a series of basic dyes. The effect may be pronounced due the compatibility of the cavity size of the extractant and that of the dye. Furthermore, the pronounced interaction may be

due to the π–π interaction between the aromatic rings, Van der Wall's forces involving methyl groups as well as hydrogen bonds between carboxylic and hydroxyl groups of the dye and the carrier **1**.

3.1.1. Effect of pH on the receiving phase

The uptake efficiency of the receiving phase was optimized by agitating 10 mL of carrier **1** (1×10^{-3} M) in chloroform containing MR with 10 mL of deionized water (receiving phase) at pH varying from 2 to 12, as shown in Fig. 3. It can be inferred from Fig. 3 that with increasing pH, the decomplexation percent of MR from carrier **1** increases and attains its maximum at pH 12. This effect may be explained by the fact that at acidic and neutral pH, the protons are left intact in the complexation phenomenon; however, at very alkaline pH values, both carrier **1** and dye molecule are losing protons, which become the active components in the complexation phenomenon. Therefore, pH 12 is favorable for back-extraction of MR from the organic phase containing carrier **1**.

3.1.2. Effect of salt as interfering species on dye transport

The use of chemical substances during the process of dyeing, printing, desizing, and finishing processes in textile industries affect the quality of industrial wastewaters. Na$_2$SO$_4$ (10–20%) is generally added to the system as an electrolyte when uniformity of the dye colour is needed for the fiber. Likewise, NaCl is utilized during the different processes in the textile and other industries. Therefore, the study was focused to evaluate the competition/interfering effect of electrolytes on the transport of MR. Therefore, three salts (NaCl, Na$_2$CO$_3$ and Na$_2$SO$_4$) at varying concentrations ranging from 1 to 50 g/L were studied as shown in Fig. 4. It could be observed from Fig. 4 that the addition of the different concentrations of NaCl and Na$_2$SO$_4$ does not affect the extraction efficiency of carrier **1**. However, in the case of Na$_2$CO$_3$ (a basic salt), a change in the donor phase solution pH from 5.5 to 11.3, results in a remarkable decrease in the MR extraction percent.

3.1.3. Effect of dye concentration on the extraction percent

The experiments were conducted to optimize the MR concentration by diluting the stock solution of MR from
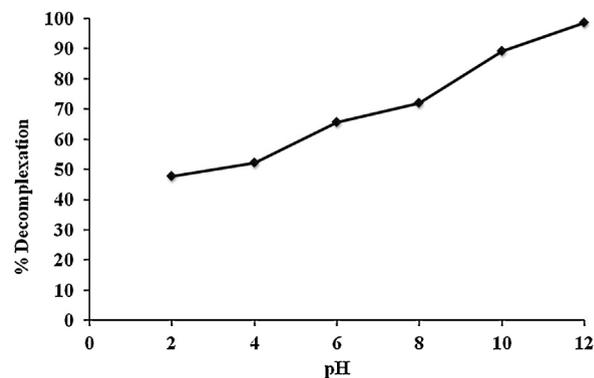
Fig. 3. Decomplexation percent of MR into the receiving phase at different pH values.
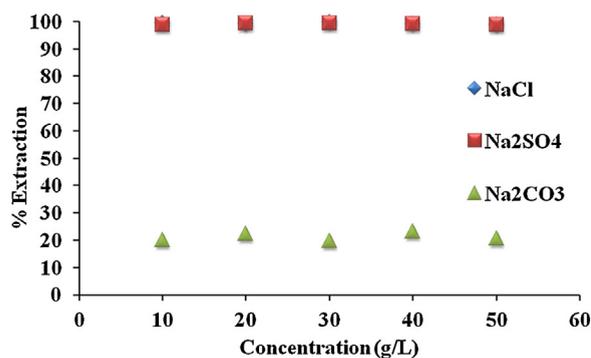
Fig. 4. Effect of interfering species on the extraction percent of MR from an aqueous phase to an organic phase containing carrier **1**.

1×10^{-6} to 1×10^{-4} M. The solutions were agitated with carrier **1** in chloroform at room temperature for 30 min. Fig. 5 reveals a sudden increase in the MR extraction percent at concentrations from 1×10^{-6} to 2.5×10^{-5} M, value for which it attains its maximum and then remains constant up to 1×10^{-4} M. This rapid enhancement in extraction percent may be explained by the fact that with increasing concentration, the contact between MR and carrier **1** is increased, and at concentration 2.5×10^{-5} M, carrier **1** gets saturated and attains a maximum extraction percent, whereas at higher concentration, carrier **1** becomes fully saturated and cannot transport MR much efficiently from the aqueous to the organic phase. Therefore, 2.5×10^{-5} M concentration was optimized for the transport of MR using carrier **1** through BLM.

3.2. Bulk liquid membrane

3.2.1. Kinetic procedure

Kinetics for the transport of MR was directly determined in the donor and receiving phase using spectro-

photometry at regular intervals of 15 min. Consequently, carrier concentration, stirrer speed and type of solvent were studied in detail through BLM. The subsequent change in concentration of dye was determined from the material balance between two phases, i.e.:

$$R_d + R_m + R_a = 1 \tag{3}$$

where R_d is the dimensionless reduced concentration of dye in the donor, R_m that in the membrane, and R_a that in the acceptor phase. The values of these parameters are calculated from the following equation.

$$R_d = \frac{C_d}{C_{d_0}} \cdot R_m = \frac{C_m}{C_{d_0}} \cdot R_a = \frac{C_a}{C_{d_0}} \tag{4}$$

where C_{d_0} is the initial dye concentration in the donor phase.

The kinetic scheme for consecutive reaction systems can be described by the following rate equations:

$$\frac{dR_d}{dt} = -k_1 R_d \equiv J_d \tag{5}$$

$$\frac{dR_m}{dt} = k_1 R_d - k_2 R_m \tag{6}$$

$$\frac{dR_a}{dt} = k_2 R_m = J_a \tag{7}$$

where J is the flux, when $k_1 \neq k_2$, and integrating the above differential equations, we have:

$$R_d = \exp(-k_1 t) \tag{8}$$

$$R_m = \frac{k_1}{k_2 - k_1} [\exp(-k_1 t) - \exp(-k_2 t)] \tag{9}$$

$$R_a = 1 - \frac{k_1}{k_2 - k_1} [k_2 \exp(-k_1 t) - k_1 \exp(-k_2 t)] \tag{10}$$
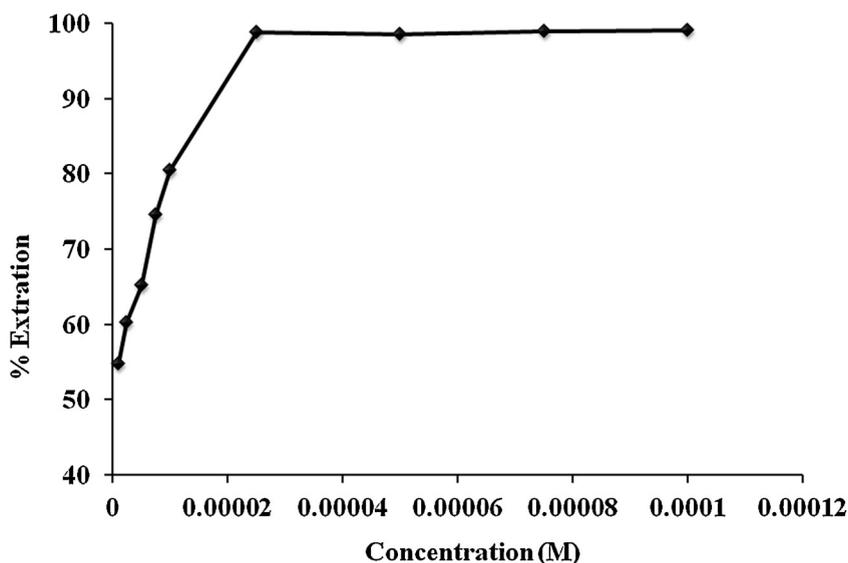
Fig. 5. Effect of different concentrations of MR on the extraction percent from an aqueous phase to an organic phase.

while the maximum values of R_m and t_{max} (when $dR_m/dt = 0$) can be written as:

$$R_m^{max} = \left(\frac{k_1}{k_2}\right)^{-k_2/(k_1-k_2)} \tag{11}$$

$$t_{max} = \left(\frac{1}{k_1-k_2}\right)\ln\frac{k_1}{k_2} \tag{12}$$

combining eqs. (11) and (12), the following relationship can be obtained.

$$k_2 = \frac{\ln\left(\frac{1}{R_m^{max}}\right)}{t_{max}} \tag{13}$$

Numerical analysis by non-linear curve fitting allows us to determine the rate constants, the value of k_1 being directly obtained by iteration from eq. (8). This value is introduced as a constant value in eqs. (9) and (10). An initial value of k_2 is obtained from eq. (13) and introduced in eqs. (9) and (10), and iterated.

By considering the first-order time differentiation – eqs. (8)–(10) – at t_{max}, one obtains the following equations:

$$\left.\frac{dR_d}{dt}\right|_{max} = -k_1\left(\frac{k_1}{k_2}\right)^{-k_1/(k_1-k_2)} \equiv J_d^{max} \tag{14}$$

$$\left.\frac{dR_a}{dt}\right|_{max} = k_2\left(\frac{k_1}{k_2}\right)^{-k_2/(k_1-k_2)} \equiv J_a^{max} \tag{15}$$

$$\left.\frac{dR_m}{dt}\right|_{max} = 0 \tag{16}$$

$$-\left.\frac{dR_d}{dt}\right| = \left.\frac{dR_a}{dt}\right| \tag{17}$$

It may be noted that at $t = t_{max}$, the system is in a steady state because the concentration of dye in the membrane does not change with time (eq. (16)). As a result, the exit and entrance fluxes are equal and have opposite signs (eq. (17)).

It can be seen that plotting R_d versus t yields a decreasing mono-exponential curve, whereas the time variation of both R_m and R_a is bi-exponential. The actual numerical analysis was carried out by non-linear curve fitting. Fig. 6 shows the variation of R_d, R_m and R_a with time through BLM.

3.2.2. Effect of solvent

The organic solvent plays an influential role in BLM transport. The distinguishing properties that a solvent must possess for better BLM transport are viscosity, water miscibility, polarity, and volatility. An appropriate
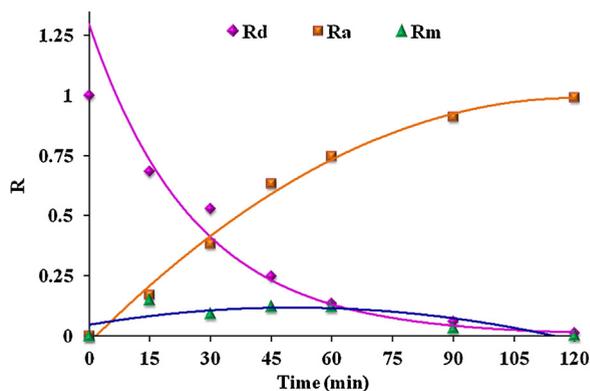
Fig. 6. (Color online.) Time dependence of R_d, R_m and R_a for the transport of the MR membrane phase: 1×10^{-3} M carrier in chloroform, stirring rate: 800 rpm at 298 K.

membrane solvent should be less viscous, less volatile, water immiscible and more polar. Solvent viscosity, volatility and water immiscibility aids in BLM stability for a long run; however, solvent polarity stabilizes polar molecules and as a result accelerates BLM transport. Thus, in the present study, $CHCl_3$, CH_2Cl_2, and CCl_4 are examined as membrane solvent to investigate their impact on BLM transport. For this study, carrier concentration, stirring rate and acceptor phase pH was set as: 1×10^{-3} M, 800 rpm and at pH 12. The results are compiled in Table 1 and Fig. 7a and b. It can be seen from the results that maximum transport of MR occurs in CH_2Cl_2 as a solvent and membrane entrance and exit rate constants increase in the order: $CCl_4 < CHCl_3 < CH_2Cl_2$. The success of using CH_2Cl_2 as a BLM membrane solvent lies in the fact that it is more polar and less viscous in comparison to both $CHCl_3$ and CCl_4. The results are also consistent with the physicochemical properties of the solvents given in Table 2.

3.2.3. Effect of stirring speed

Stirring speed plays a very important role in dye transportation between the two phases. Therefore, our study was conducted by changing the stirring rates of the membrane phase from 200, 400, 600 and 800 rpm at 298 K using 1×10^{-3} M of carrier **1** in CH_2Cl_2. The results are compiled in Table 3 and Fig. 8a. The increase in flux (k_1 and k_2) and the decrease in t_{max} values, suggesting that maximum transport efficiency of MR occurs at higher stirring speed; this might be due to the fact that higher stirring rates helps mixing donor and receiving phases by minimizing the concentration polarization in the donor phase and by enhancing the penetrating power of MR in the receiving phase. Accordingly, the transport efficiency

Table 1
Kinetic parameters of MR in different solvents.

Solvent	$k_1 \times 10^2$ (min^{-1})	$k_2 \times 10^2$ (min^{-1})	R_m^{max}	t_{max} (min)	$J_d^{max} \times 10^2$ (min^{-1})	$J_a^{max} \times 10^2$ (min^{-1})	Dye transported (%)
$CHCl_3$	1.9	7.5	0.11	30	−1.2	1.2	97
CH_2Cl_2	3.8	12.7	0.15	15	−2.3	2.3	99
CCl_4	0.4	1.8	0.037	180	−0.3	0.3	64
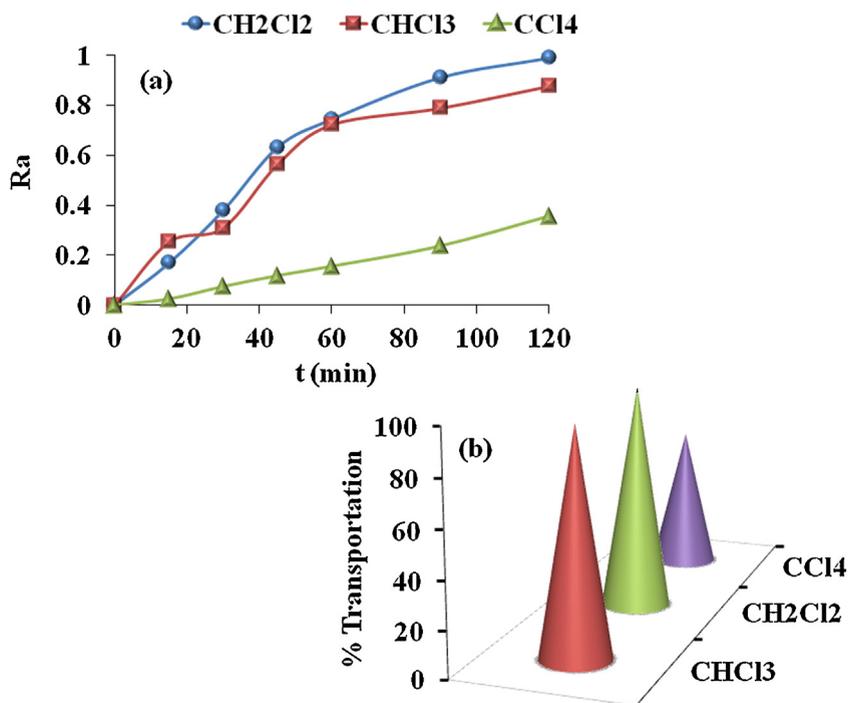
Fig. 7. (Color online.) a. R_a variation vs. time. b. Percentage transportation for the transport of MR in different solvents.

Table 2
Physicochemical characteristics of solvents [10].

Solvent	ε_o	n_D	μ	η	V_m
CH_2Cl_2	9.08	1.42	1.96	0.44	64.2
$CHCl_3$	4.81	1.45	1.35	0.58	96.5
CCl_4	2.24	1.47	0	0.97	96.5

ε_o: dielectric constant (20 °C); n_D refractive index (20 °C); μ dipole moment (D); η viscosity (cP); V_m molar volume (M).

of MR through BLM decreases with a lower stirring rate. In the present study, 99% of the MR is transported to the receiving phase at 800 rpm (Fig. 8b).

3.2.4. Effect of carrier concentration

The important component of BLM carrier is that removes the active component from donor phase by complexing with it and after subsequent diffusion into organic phase; it discharges that component into the receiving phase. Therefore, it is compulsory to optimize the carrier concentration that can efficiently transport the maximum quantity of the active component. Thus, transport experiments were conducted by diluting the stock solution of carrier **1** from 1×10^{-3} to 1×10^{-5} M in CH_2Cl_2 at 298 K and 800 rpm. The results (Table 4 and

Fig. 9a–c) demonstrate that with increasing the dye concentration regularly increases the MR flux values. Equations (6) and (7) also reveal the dependence of flux values on concentration. This might be due to the fact that the carrier saturation at the interface between the donor and receiving phase does not occur at lower concentrations. However, the experiments were also performed without carrier in order to optimize the effect of the solvent. Results obtained showed no appreciable MR movement through BLM; therefore, the additional effect was assumed to be due to carrier **1**.

3.3. Lifetime of the bulk liquid membrane

The lifetime of BLM was observed for multiple cycles and MR dye was transported through BLM under optimum conditions. The transportation percent of the dye after 15 min using five replicates of bulk liquid membrane solution was observed to be $99 \pm 1\%$.

3.4. Transport mechanism

The phenomenon governing MR transport from the donor phase to the receiving phase through the organic

Table 3
Kinetic parameters of MR at different stirring rates (solvent CH_2Cl_2; T = 298 K).

Stirring rate (rpm)	$k_1 \times 10^2$ (min^{-1})	$k_2 \times 10^2$ (min^{-1})	R_m^{max}	t_{max} (min)	$J_d^{max} \times 10^2$ (min^{-1})	$J_a^{max} \times 10^2$ (min^{-1})	Dye transported (%)
200	0.9	2.3	0.066	120	−0.5	0.5	63
400	2.0	4.2	0.078	60	−1.0	1.0	81
600	3.1	5.6	0.082	45	−1.5	1.5	95
800	3.8	12.7	0.15	15	−2.3	2.3	99
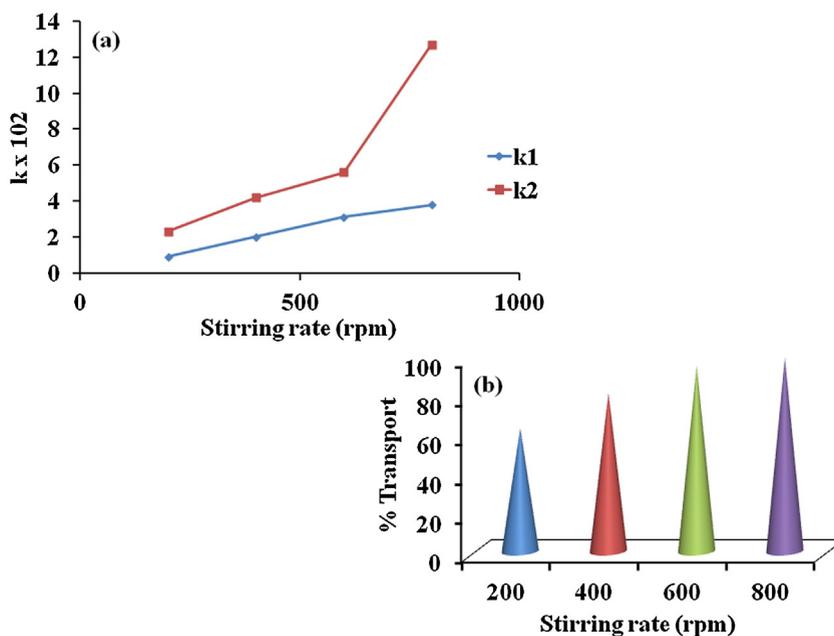
Fig. 8. (Color online.) Effect of stirring rate on (a) flux values, (b) transportation percent of MR through BLM.

Table 4
Effect of carrier **1** concentration on the kinetic parameters governing the transport of MR (solvent: CH_2Cl_2, 298 K, and 800 rpm).

Conc.	$k_1 \times 10^2$ (min^{-1})	$k_2 \times 10^2$ (min^{-1})	R_m^{max}	t_{max} (min)	$J_d^{max} \times 10^2$ (min^{-1})	$J_a^{max} \times 10^2$ (min^{-1})	Dye transported (%)
1×10^{-5}	1.0	2.0	0.049	150	−0.5	0.5	73
1×10^{-4}	2.3	3.1	0.060	90	−1.0	1.0	91
1×10^{-3}	3.8	12.7	0.15	15	−2.3	2.3	99
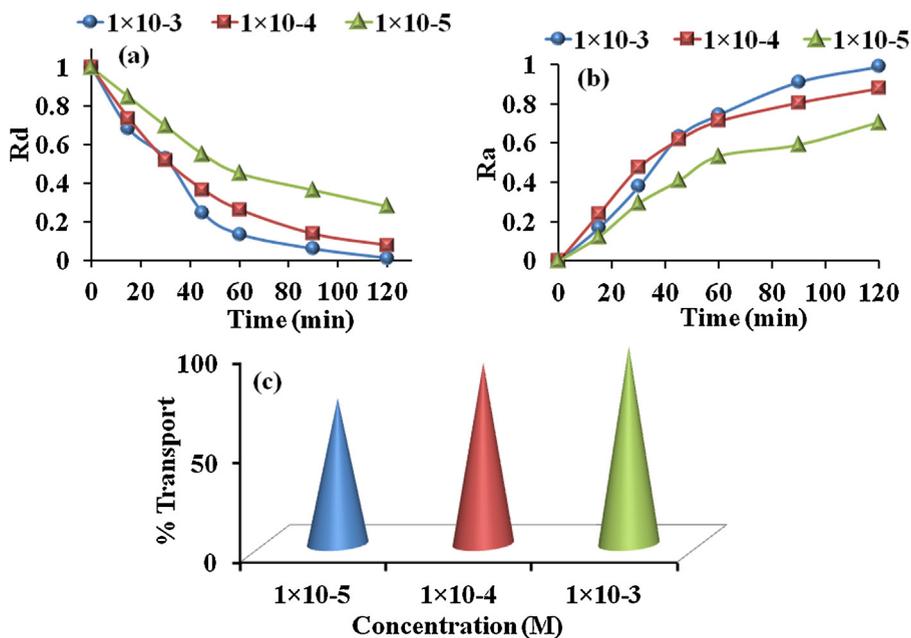
Fig. 9. (Color online.) Time variation of reduced concentrations (a) R_a, (b) R_d and (c) transportation percent of MR transported through BLM at different carrier concentrations in CH_2Cl_2.
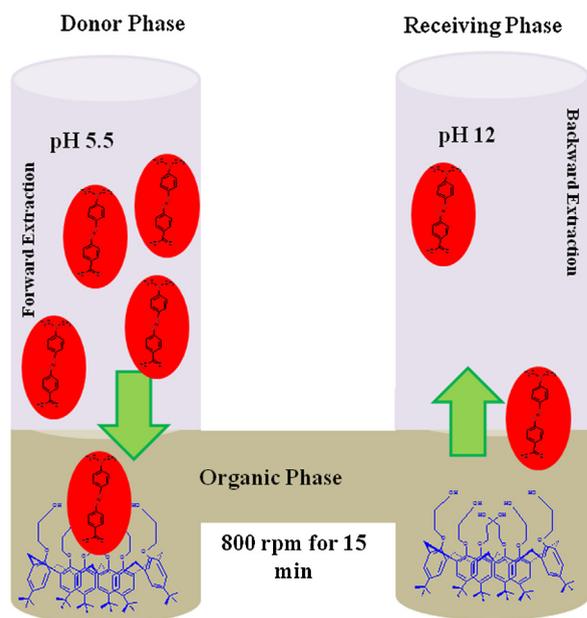
Fig. 10. (Color online.) Transport mechanism of MR from the donor to the receiving phase through BLM using carrier **1**.

phase containing carrier **1** (Fig. 10) can be explained as follows.

The first step involves the diffusion of MR from the donor to the membrane interface through the aqueous boundary layer by complexation between MR and carrier **1**. This may be due to intermolecular interactions, including π–π interactions, van der Waals forces as well as hydrogen bonding, as described in Section 3.1. In the second step, the movement of complex through the membrane towards the receiving phase is due to the potential gradient developed between the donor and carrier phases. However, at the junction between the membrane and the acceptor phase, decomplexation of the carrier MR takes place, due to the alkaline pH of the receiving phase, where both MR molecule and carrier **1** are losing protons, resulting in a successive and efficient release of MR into the receiving phase. Finally, the carrier is free of MR and diffuses back into the organic membrane to carry another MR molecule; the cycle continues till 99% transfer of MR successfully takes place.

3.5. Application to real wastewater samples

The developed BLM method was applied on a real wastewater sample collected in the vicinity of Jamshoro industrial area. Under optimum conditions, 10 mL of this sample solution were taken as the donor phase and transferred into the receiving phase through BLM using

Table 5
Transport of MR in real and experimental samples through BLM.

Sample	Remained (%)	Transported (%)
Real sample 1	0.5	99.5
Real sample 2	0.1	99.9

Table 6
Comparative study of carrier (**1**) with other carriers used for different dyes.

Carrier	Dye	Time taken for removal (min)	% removal	Reference
D$_2$EHPA/M$_2$EHPA and sesame oil	Methylene blue	420	62	[14]
Tetra butyl ammonium bromide	Cibacron red FN-R	70	95 ± 0.1	[15]
Cyanex 301	Methylene blue	420	85	[16]
Cationic carrier	Anionic dyes	70	97 ± 2	[17]
Calix[6]arene based derivative	Methyl red	15	99	Present study

carrier **1**. The sample was analyzed by UV–visible spectrophotometry to check the absorbance before its transport through BLM. The results in Table 5 reveal that carrier **1** can efficiently transport MR present in the real sample.

3.6. Comparative study

The developed carrier **1**-based BLM can be compared in its efficiency with the previously reported carriers (Table 6). It can be revealed from the table that the new developed calix[6]arene based carrier is least time consuming and highly efficient for the transport of dye as compared to previously reported carriers for BLM.

4. Conclusion

In this paper, the kinetic transfer of methyl red via bulk liquid membrane using **1** as excellent and selective carrier is elaborated. The MR extraction efficiency is influenced by many factors, including initial dye concentration, acceptor phase pH, and carrier concentrations in the membrane phase, type of solvent and stirring rate. Moreover, mass transfer of MR is not affected by the presence of electrolytes, such as NaCl and Na$_2$SO$_4$. However, the addition of Na$_2$CO$_3$ causes a significant decrease in the mass transfer of MR. The kinetics of MR transport across BLM is accomplished on the basis of a scheme implying two consecutive irreversible first-order reactions. The membrane entrance (k_1) and exist rate (k_2) constants and membrane interfacial transport fluxes of extraction (J_d^{max}) and re-extraction (J_a^{max}) were also determined. The set of optimum experimental conditions for maximum MR transport (99%) through BLM is as follows: donor phase dye concentration: 2.5×10^{-5} M, carrier concentration: 10^{-3} M, membrane solvent: CH$_2$Cl$_2$, acceptor phase pH: 12, stirring rate: 800 rpm. The proposed BLM is also applied successfully to the treatment of textile industrial wastewater. Conclusively, this simple and efficient method provides remarkable advantages in terms of dye removal efficiency, cost and handling among various applied contemporary techniques. However, it needs some technical improvements for large-scale commercial applications. In this regard, the expected difficulties that can be

encountered are the choice of non-corrosive material that can be aligned inside the cell so that, when working in a wide range of pH (2–12), the cell remains safe. Furthermore, BLMs have low interfacial surface areas; consequently, for large-scale applications, the cell should be designed in such a way so that interfacial surface area can be increased to facilitate the transfer of large amount of wastewater.

Acknowledgment

References

[1] S. Patil, S. Renukdas, N. Patel, Int. J. Environ. Sci. 1 (2011) 711.
[2] Student Safety Sheets, Dyes & Indicators©CLEAPSS, 2007.
[3] G.M. Nisola, E. Chb, A.B. Beltran, M. Han, Y. Kim, W.J. Chung, Chemosphere 80 (2010) 894.
[4] M. Turabik, B. Gozme, Clean–Soil, Air, Water 41 (2013) 1080, http://dx.doi.org/10.1002/clen.201200220.
[5] W.J. Lau, A.F. Ismail, Desalination 245 (2009) 321.
[6] M. Gharehbaghi, F. Shemirani, Clean–Soil, Air, Water 40 (2012) 290.
[7] A. Razaee, M.T. Ghaneian, S.J. Haashemian, G.H. Moussavi, G.H. Ghanizadeh, E. Hajizadeh, Iran, J. Environ. Health Sci. Eng. 5 (2008) 95.
[8] T. Poursaberi, M. Hassanisadi, Clean–Soil, Air, Water 41 (12) (2013) 1208.
[9] T. Robinson, G. McMullan, R. Marchant, P. Nigam, Bioresour. Technol. 77 (2001) 247.
[10] M. Ersoz, Adv. Colloid Interface Sci. 134–135 (2007) 96.
[11] I. Zaharia, I. Diaconu, E. Ruse, G. Nechifor, J. Nanomat. Biostruct. 7 (2012) 1303.
[12] T. Alizadeh, N. Memarbashi, Sep. Purif. Technol. 90 (2012) 83.
[13] R. Tandlich, Application of Liquid Membranes in Wastewater Treatment, in: V.S. Kislik (Ed.), Liquid Membranes Principles and Applications in Chemical Separations and Wastewater Treatment, Elsevier B.V, 2010, Chapter 8, pp. 357–400.
[14] P. Kazemi, M. Peydayesh, A. Bandegi, T. Mohammadi, O. Bakhtiari, Chem. Papers 67 (2013) 722.
[15] G. Muthuraman, M. Ibrahim, J. Ind. Eng. Chem. 19 (2) (2013) 444.
[16] S.S. Madaeni, Z. Jamali, N. Islami, Sep. Purif. Technol. 81 (2011) 116.
[17] G. Muthuraman, K. Palanivelu, J. Sci. Ind. Res. 64 (2005) 529.
[18] N. Hajarabeevi, I.M. Bilal, D. Easwaramoorthy, K. Palanivelua, Desalination 245 (2009) 19.
[19] G. Muthuraman, T.T. Teng, Desalination 249 (2009) 1062.
[20] C. Das, M. Rungta, G. Arya, S. Dasgupta, S. De, J. Hazard Mater. 159 (2008) 365.
[21] N. Othman, S.N. Zailani, N. Mili, J. Hazard Mater. 198 (2011) 103.
[22] H.K. Alpoguz, A. Kaya, S. Memon, M. Yilmaz, J. Macromol. Sci. Pure Appl. Chem. 44 (2007) 17.
[23] F.T. Minhas, S. Memon, I. Qureshi, M. Mujahid, M.I. Bhanger, C. R. Chimie 16 (2013) 742.
[24] J.K. Moran, E.M. Georgiev, A.T. Yordanov, J.T. Mague, D.M. Roundhill, J. Org. Chem. 59 (1994) 5990.
[25] J. Pedersen, Fed. Proc., Fed. Am. Soc. Exp. Biol. 27 (1968) 1305.